






## Contribution to the Themed Section: 'a Tribute to the Life and Accomplishment of Sidney J. Holt'

# Accounting for non-stationary stock–recruitment relationships in the development of MSY-based reference points

Fan Zhang <sup>1\*</sup>, Paul M. Regular <sup>2</sup>, Laura Wheeland <sup>2</sup>, Rick M. Rideout<sup>2</sup>, and M. Joanne Morgan<sup>2</sup>

<sup>1</sup>Centre for Fisheries Ecosystems Research, Fisheries and Marine Institute, Memorial University of Newfoundland, St. John's, NL A1C 5R3, Canada

<sup>2</sup>Northwest Atlantic Fisheries Centre, Fisheries and Oceans Canada, P.O. Box 5667, St. John's, NL A1C 5X1, Canada

\*Corresponding author: tel: (+1)709-778-0634; e-mail: [fan.zhang@mi.mun.ca](mailto:fan.zhang@mi.mun.ca).

Zhang, F., Regular, P. M., Wheeland, L., Rideout, R. M., and Morgan, M. J. Accounting for non-stationary stock–recruitment relationships in the development of MSY-based reference points. – ICES Journal of Marine Science, 78:2233–2243.

Received 20 May 2020; revised 1 September 2020; accepted 2 September 2020; advance access publication 30 October 2020.

Stock–recruitment relationships (SRRs) may vary over time due to ecological and anthropogenic impacts, challenging traditional approaches of calculating maximum sustainable yield (MSY)-based reference points that assume constant population traits. We compare seven methods to calculate MSY,  $F_{MSY}$  and  $B_{MSY}$  by modelling constant, stochastic (uncorrelated), and autocorrelated SRRs using simulations and two case studies [Atlantic cod (*Gadus morhua*) and American plaice (*Hippoglossoides platessoides*) on the Grand Bank off Newfoundland, Canada]. Results indicated that the method used to model SRRs strongly affected the temporal pattern of recruitment projection, and the variations generated by autocorrelated SRRs were more similar to observed patterns. When the population productivity had low-frequency and large-magnitude variations, stochastic SRRs generated greater MSY and  $F_{MSY}$  estimates than constant or autocorrelated SRRs, while no consistent pattern of  $B_{MSY}$  was detected. In the case studies, stochastic and autocorrelated SRRs produced asymmetric relationships between fishing mortality and yield, with higher risk of overfishing by going beyond  $F_{MSY}$ . Overall, our results suggest that caution should be taken when calculating MSY-based reference points in highly dynamic ecosystems, and correctly accounting for non-stationary population dynamics could, therefore, lead to more sustainable fisheries.

**Keywords:** American plaice, Atlantic cod, MSY, non-stationary population process, reference point, stock–recruitment relationship

## Introduction

Maximum sustainable yield (MSY) is a fundamental concept in fisheries management that has been applied throughout the world to define fisheries status and calculate management reference points (Beverton and Holt, 1957). For example,  $F_{MSY}$  and  $B_{MSY}$  (i.e. the fishing mortality and biomass leading to MSY) are two widely used reference points to define the “overfishing” and “overfished” status of fisheries. The concept of MSY is originally derived from the equilibrium dynamics of surplus production models (Beverton and Holt, 1957). That is, MSY is achieved when a fish stock is fished down to half the size of the stock's carrying capacity. In age-structured stock assessments, MSY is

typically calculated by simulating long-term stock dynamics under different fishing mortalities using pre-defined key population traits, e.g. stock–recruitment relationship (SRR), natural mortality, maturity at age, and weight at age. Under a precautionary approach (PA) to fisheries management, MSY-based reference points are often treated as limits rather than targets in harvest strategies (e.g. Mangel *et al.*, 2013). For example, Holt (2020) strongly advocated that fishing mortality should be set below  $F_{MSY}$  to reduce the risk of overexploitation while, at the same time, to maximize the profitability of fisheries.

In ecosystems where biotic and environmental conditions show large changes over time, key population traits can exhibit

periodic, directional, or regime-like changes (Thorson *et al.*, 2015; Szuwalski and Hollowed, 2016). For example, decadal changes in climate and oceanographic effects (Peterman and Dornier, 2012), species invasions (Zhang *et al.*, 2018), or fisheries-induced changes to population age structure (Hidalgo *et al.*, 2014) have led to changes over time in SRRs for several marine and freshwater fish populations (Walters, 1987). The emergence of non-stationary SRRs challenges the validity of traditional approaches that calculate MSY using constant population traits and calls for novel methods to calculate MSY-based reference points in highly dynamic ecosystems. One option is to use average population traits estimated only under the “prevailing” environmental conditions (e.g. estimate  $F_{MSY}$  based on stock–recruitment data under only the current ecosystem conditions). However, there are several challenges with this approach: (i) ecosystem regimes or prevailing conditions are difficult to define and detect (Klaer *et al.*, 2015); (ii) using a subset of historic data could reduce the precision of model estimations due to smaller sample size; and (iii) future conditions and population dynamics may continue to change and, therefore, reduce the effectiveness of these MSY-based reference points. Another option is to use long-term simulations that account for time-varying population traits. For example,  $F_{MSY}$  may be defined as the fishing mortality achieving maximum long-term yield by simulating population dynamics with time-varying SRRs. This approach does not require identifying, understanding, or projecting ecosystem changes that affect fish recruitment dynamics; neither does it require shortening historic data. Nevertheless, challenges remain on how to model time-varying SRRs in realistic ways.

In this study, we compare MSY,  $F_{MSY}$ , and  $B_{MSY}$  using seven methods to model SRRs: (i) constant SRR over the whole available time-period (SRR-whole), (ii) constant SRR over recent period (SRR-recent), (iii) stochastic SRRs with white noise (SRR-noise), (iv) stochastic SRRs by resampling historical values (SRR-resample), (v) autocorrelated SRRs with first-order autoregressive (AR1) variations (SRR-AR1), (vi) autocorrelated SRRs with cut-off at historical maximum and minimum values (SRR-cut-off), and (vii) autocorrelated SRRs bounded by historical maximum and minimum values (SRR-bounded). We compare the seven methods using both simulation and case studies. In the simulation, we compare different methods under four scenarios of productivity variations: (i) stochastic variation, (ii) upward shift, (iii) downward shift, and (iv) collapse and recover (Figure 1). In the case studies, we focus on two fish stocks on the Grand Bank off Newfoundland: Northwest Atlantic Fisheries Organization (NAFO) Divisions 3NO Atlantic cod (*Gadus morhua*) and 3LNO American plaice (*Hippoglossoides platessoides*), hereafter referred to as 3NO cod and 3LNO plaice (Figure 2). Atlantic cod and American plaice on the Grand Bank supported historically important commercial fisheries; however, both stocks collapsed in the early 1990s and have been under a moratorium to directed fishing since 1994 (Rideout *et al.*, 2018; Wheeland *et al.*, 2018). These dramatic population changes coincided with strong variation in the SRRs for both fish stocks (Morgan *et al.*, 2014).

## Methods

### Time-invariant and time-varying SRRs

The SRR is modelled by the classic Ricker model (Ricker, 1954). To model time-invariant and time-varying SRRs, two forms of

Ricker models are used (Table 1): a basic form with time-invariant parameters (*Ricker*) and a modified form with time-varying parameters (*Ricker.tv*). In the *Ricker* model, parameters are constant and combined measurement and process errors are distributed following a lognormal distribution. In the *Ricker.tv* model, the productivity parameter follows an AR1 variation (i.e. represent AR1 process errors) and measurement errors follow a lognormal distribution. In both models, measurement and process errors are confounded. To separate these, the standard deviation of measurement error is assumed to be 0 in the simulation study (i.e. no measurement error of recruitment) and fixed at 0.3 in the case study based on the observed variance of survey recruitment indices. The parameters of stock–recruitment models are estimated using Template Model Builder (Kristensen *et al.*, 2016).

### Seven methods to model SRRs

When calculating MSY-based reference points, the SRR parameter estimates (Table 2) are used to model the variations in SRRs via seven methods: SRR-whole, SRR-recent, SRR-noise, SRR-resample, SRR-AR1, SRR-cut-off, and SRR-bounded.

#### SRR-whole

The *Ricker* model is fitted to all historical stock–recruitment data. SRR is modelled without process errors using the estimated values of  $\alpha$  and  $\beta$ .

#### SRR-recent

The *Ricker* model is fitted to the stock–recruitment data in recent years. SRR is modelled without process errors using the estimated values of  $\alpha$  and  $\beta$ .

#### SRR-noise

The *Ricker* model is fitted to all historical stock–recruitment data. SRR is modelled using the estimated values of  $\alpha$  and  $\beta$ , with white-noise error (i.e. errors are distributed normally with mean zero and standard deviation equals the estimated value of  $\sigma_p$ ).

#### SRR-resample

The *Ricker.tv* model is fitted to all historical stock–recruitment data. SRR is modelled using the estimated values of  $\beta$ , and  $a_t$  is randomly sampled with replacement from the estimated historical values.

#### SRR-AR1

SRR-AR1 is same as SRR-resample, except that  $a_t$  follows an AR1 process that converges to the historical mean and variance.

Let  $\mu_{hist}$  and  $\sigma_{hist}$  denote the mean and variance of the historically estimated values of  $a_t$ . To have a stationary distribution converge to  $\mu_{hist}$  and  $\sigma_{hist}$  the projected  $a_t$  should follow the AR1 process,

$$a_t = \mu_{hist} \times (1 - \varphi_a) + \varphi_a \times a_{t-1} + \varepsilon_t,$$

$$\varepsilon_t \sim N\left(0, \sigma_{hist} \times \sqrt{1 - \varphi_a^2}\right),$$

where  $\varphi_a$  is fixed at values estimated from *Ricker.tv*.

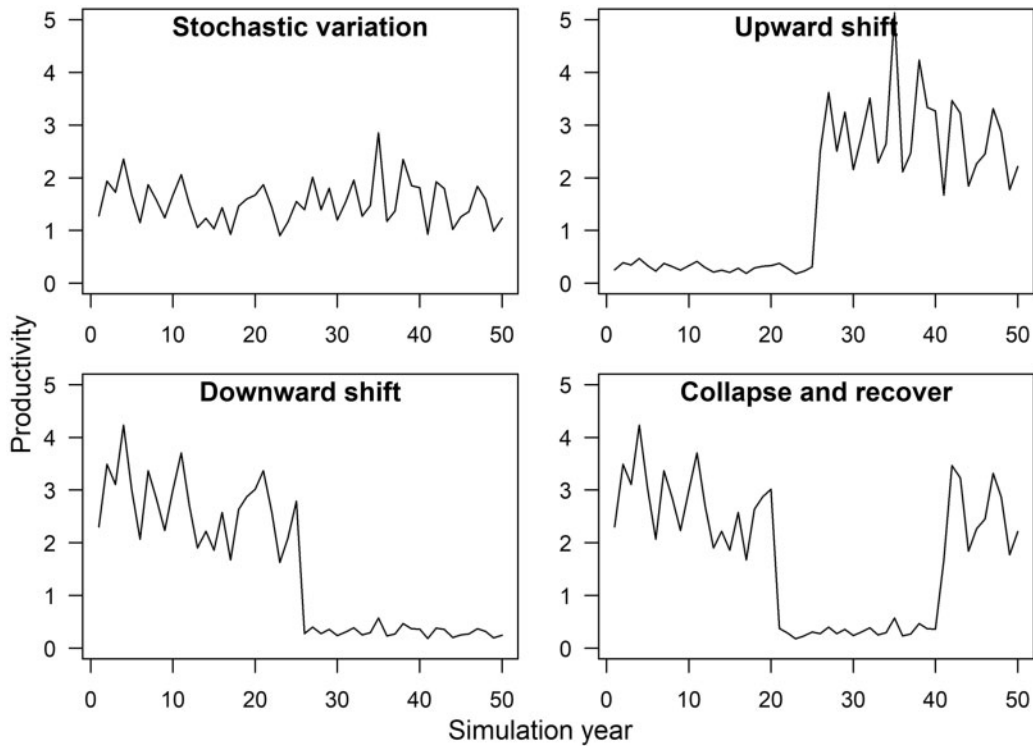


**Figure 1.** Four scenarios of productivity (represented by  $\alpha_t$  in Ricker model) variation in the operating module. Scenario 1: stochastic variation; scenario 2: upward shift; scenario 3: downward shift; and scenario 4: collapse and recover.

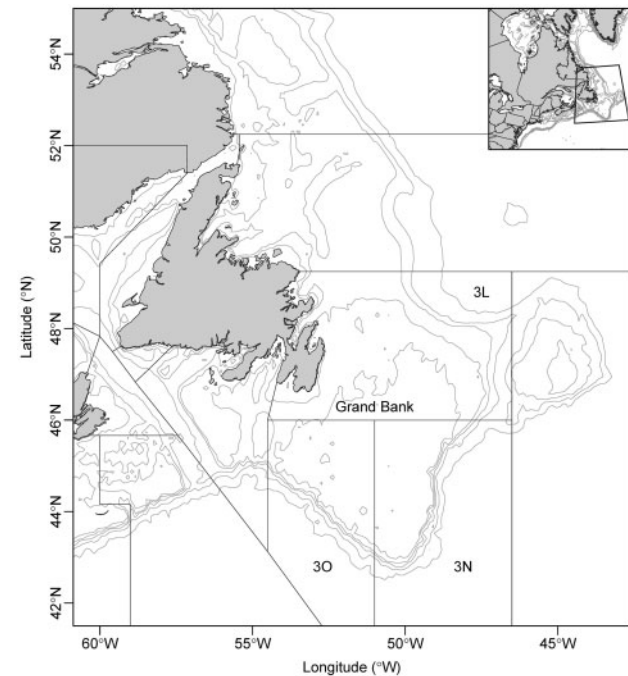


**Figure 2.** Study area and management units of Atlantic cod and American plaice on the Grand Bank.

**SRR-cut-off**

SRR-cut-off is same as SRR-AR1, except that  $a_t$  is cut-off when exceeding the maximum and minimum values of historical estimates:

Let  $a_{max}$  and  $a_{min}$  be the maximum and minimum values of the  $a_t$  estimated from *Ricker\_tv*,

$$a_t = \begin{cases} a_{max} & \text{(if } a_t \geq a_{max} \text{)} \\ a_t & \text{(if } a_{max} > a_t > a_{min} \text{)} \\ a_{min} & \text{(if } a_t \leq a_{min} \text{)} \end{cases}$$

**SRR-bounded**

SRR-bounded is same as SRR-resample, except that  $a_t$  follows an AR1 process and is bounded by historical maximum and minimum values using logit-linear transformation.

A four-step process is used to construct a time series  $a_t$  that contains an AR1 process with specified autocorrelation coefficient  $\phi_a$ , converges to stationary distribution with mean  $\mu_{hist}$  and standard deviation  $\sigma_{hist}$ , and also bounded by  $a_{max}$  and  $a_{min}$ .

Step 1: let  $z_t = \frac{a_t - a_{min}}{a_{max} - a_{min}}$ , then  $z_t$  is bounded by (0,1),  $E(z_t) = \frac{\mu_{hist}}{a_{max} - a_{min}}$ , and  $var(z_t) = \frac{\sigma_{hist}^2}{(a_{max} - a_{min})^2}$ .

Step 2: let  $y_t = \text{logit}(z_t)$ , then  $y_t$  follows a normal distribution with mean  $\mu_y$  and standard deviation  $\sigma_y$ . Find the values of  $\mu_y$  and  $\sigma_y$  through numerical optimization using *logitnorm* package in R (Wutzler, 2018).

Step 3: construct a time series  $y_b$  so that  $y_t$  follows an AR1 process with autocorrelation coefficient  $\phi_a$  and converges to stationary distribution with mean  $\mu_y$  and standard deviation  $\sigma_y$ :

$$y_t = \mu_y \times (1 - \phi_a) + \phi_a \times y_{t-1} + \varepsilon_t,$$

$$\text{where } \varepsilon_t \sim N\left(0, \sigma_y \times \sqrt{1 - \phi_a^2}\right).$$

**Table 1.** The two forms of Ricker models used to estimate stock–recruitment relationships.

Model	Function	Measurement error	Process error
Ricker	$R_t = \alpha \times S_{t-r} \times e^{\beta m_t + \varepsilon_{pt}}$	$\varepsilon_{mt} \sim N(0, \sigma_m^2)$	$\varepsilon_{pt} \sim N(0, \sigma_p^2)$
Ricker.tv	$R_t = \alpha_{t-r} \times S_{t-r} \times e^{-\beta \times S_{t-r}} \times e^{\varepsilon_{rt}}$	$\varepsilon_{rt} \sim N(0, \sigma_r^2)$	$a_t = \log(\alpha_t)$ $a_t = a + \varepsilon_{at}$ $\varepsilon_{a1}, \dots, \varepsilon_{aT} \sim MVN(0, \Sigma)$ $\Sigma$ —AR(1) covariance matrix with parameters $\sigma_a^2$ and $\rho_a$

**Table 2.** Parameters of the Ricker models.

Symbol	Definition
$R_t$	Recruitment abundance in year $t$
$S_t$	Spawning-stock biomass in year $t$
$R$	Age of recruitment
$A$	Productivity parameter of stock–recruitment relationship
$\alpha_t$	Productivity parameter of stock–recruitment relationship in year $t$
$a_t$	Logarithm of $\alpha_t$
$A$	Mean of $a_t$
$\varepsilon_{_a t}$	Residual of $a_t$
$\beta$	Density dependence parameter of stock–recruitment relationship
$\varphi_a$	Autocorrelation coefficient of $\varepsilon_{_a t}$
$\varepsilon_{_m t}$	Measurement error of recruitment in Ricker
$\varepsilon_{_p t}$	Process error of recruitment in Ricker
$\varepsilon_{_r t}$	Measurement error of recruitment in Ricker.tv
$\sigma_m$	Standard deviation of $\varepsilon_{_m t}$
$\sigma_p$	Standard deviation of $\varepsilon_{_p t}$
$\sigma_r$	Standard deviation of $\varepsilon_{_r t}$
$\sigma_a$	Standard deviation of $\varepsilon_{_a t}$

Step 4: derive the time series  $a_t$  from  $y_t$ :

$$a_t = a_{min} + \frac{e^{y_t}}{1 + e^{y_t}} \times (a_{max} - a_{min}).$$

**Calculate MSY-based reference points**

For each of the seven methods to model SRRs, three MSY-based reference points (MSY,  $F_{MSY}$ , and  $B_{MSY}$ ) are calculated using simulation. There are three layers of simulation loops (Supplementary Figure S1): the first layer loops over 100 repetitions, the second layer loops over 100 trials of fishing mortality, and the third layer loops over 500 simulation years. In the first layer, one out of 100 sets of constant and/or time-varying SRR parameters is generated based on the selected method to model SRRs. In the second layer, one out of 100 values of fishing mortality is selected (range from 0 to 1, with interval equal to 0.01). In the third layer, the population is projected for 500 years using age-based population dynamics models (Table 3). Key population variables, i.e. weight at age, maturity at age, natural mortality, and selectivity pattern, are fixed based on the average values over all historical data and assumed to be time invariant. Overall, the simulation comprises 70 000 runs, and each run generates a time series of population dynamics over 500 years.

For each run, the long-term yield and biomass are defined as the average annual yield and biomass over the last 100 simulation years. For each method to model SRRs, there are 100 repetitions of long-term yield and biomass under each level of fishing mortality, and the mean values of the long-term yield (MLY) and biomass (MLB) across 100 repetitions are calculated. Then, for each

method to model SRRs, we define MSY as the maximum MLY,  $F_{MSY}$  as the fishing mortality that maximizes MLY, and  $B_{MSY}$  as the MLB when fishing at  $F_{MSY}$ .

**Simulation study**

The simulation comprises operating and estimation modules. In the operating module, “true” population dynamics are generated using the age-based population dynamics models (Table 3). The population dynamics is simulated for 100 years, and the first 50 years are the burn-in period with constant SRR to stabilize population dynamics. In the last 50 years, four scenarios of productivity variation are modelled by changing the productivity parameter (i.e.  $\alpha_t$ ) of stock–recruitment models (Table 4). The key variables in the simulation, e.g. fishing selectivity, stock–recruitment parameter, natural mortality, maturation, and weight at age, are specified based on the population dynamics estimated for 3NO cod and assumed to be constant over time (Supplementary Table S1). Each scenario of the operating model is repeated 100 times, and in total, 400 sets of simulated data are generated.

In the estimation module, the MSY-based reference points are calculated by the seven methods to model SRRs (described above) using the last 50 years of population dynamics from each simulated dataset. For the SRR-recent method, the last 20 years are specified as the recent period.

**Case studies**

3NO cod and 3LNO plaice are assessed by the NAFO Scientific Council. The dynamics of both populations are currently estimated by virtual population analysis using the ADAPTive framework (Rideout et al., 2018; Wheeland et al., 2018). The stock assessment of 3NO cod goes back to 1959, and age 3 individuals are considered as recruitment to the fishery. The stock assessment of 3LNO plaice starts from 1960, and recruitment to the fishery is considered to be age 5. In this study, we use the model input and output data from the recent assessments of 3NO cod (1959–2017; ages 3–12) and 3LNO plaice (1960–2017; ages 5–15+), i.e. catch and stock weight at age, maturity at age, natural mortality, estimated number at age, estimated spawning-stock biomass (SSB), and estimated fishing mortality at age (Rideout et al., 2018; Wheeland et al., 2018). For the case studies, the recent period is defined as the time after moratoria (1994–2017) when using the SRR-recent method.

**Results**

**Seven methods to model SRRs**

The seven methods to model SRRs produced drastically different patterns of productivity, recruitment, and SSB (Figure 3). SRR-whole and SRR-recent projected constant productivity, and the projected recruitment and SSB reached equilibrium within 100 simulation years. SRR-noise and SRR-resample projected highly stochastic productivity, recruitment, and SSB, while the temporal variations projected by SRR-AR1, SRR-cut-off, and SRR-

**Table 3.** Age-based population dynamics model structures and parameters.

Models	Parameters
$R_t = \alpha_t \times S_{t-r} \times e^{-\beta \times S_{t-r}}$	$R_t$ and $S_t$ are the recruitment and SSB in year $t$ , $r$ is the age of recruitment, and $\alpha_t$ and $\beta$ are SRR parameters generated based on the corresponding method to model SRRs
$F_{a,t} = F_{trial} \times s_a$	$F_{a,t}$ is the fishing mortality at age $a$ in year $t$ , $F_{trial}$ is the fishing mortality specified in the second layer, and $s_a$ is the fishing selectivity at age $a$
$N_{r,t} = R_t$	$N_{a,t}$ and $M_{a,t}$ are the population abundance and natural mortality at age $a$ in year $t$
$N_{a+1,t+1} = N_{a,t} \times e^{-(F_{a,t}+M_{a,t})}$	$B_{a,t}$ and $wt_{a,t}$ are the population biomass and fish body weight at age $a$ in year $t$
$B_{a,t} = N_{a,t} \times wt_{a,t}$	$A$ is the maximum age, $mat_{a,t}$ is the proportion of matured fish at age $a$ in year $t$
$S_t = \sum_{a=r}^A B_{a,t} \times mat_{a,t}$	$C_{a,t}$ is the catch biomass at age $a$ in year $t$
$C_{a,t} = \frac{F_{a,t}}{F_{a,t}+M_{a,t}} \times N_{a,t} \times (1 - e^{-F_{a,t}}) \times wt_{a,t}$	$Y_t$ is the fisheries yield in year $t$
$Y_t = \sum_{a=r}^A C_{a,t}$	

**Table 4.** Variations in productivity in the four scenarios of operating module.

Scenario	Variation of $\alpha_t$
Stochastic variation	$\alpha_t = \alpha_{medium} \times e^{\epsilon_t}$
Upward shift	$\alpha_t = \begin{cases} \alpha_{low} \times e^{\epsilon_t} & (t \leq 25) \\ \alpha_{high} \times e^{\epsilon_t} & (t > 25) \end{cases}$
Downward shift	$\alpha_t = \begin{cases} \alpha_{high} \times e^{\epsilon_t} & (t \leq 25) \\ \alpha_{low} \times e^{\epsilon_t} & (t > 25) \end{cases}$
Collapse and recover	$\alpha_t = \begin{cases} \alpha_{high} \times e^{\epsilon_t} & (t \leq 20) \\ \alpha_{low} \times e^{\epsilon_t} & (20 < t \leq 40) \\ \alpha_{high} \times e^{\epsilon_t} & (t > 40) \end{cases}$

$\epsilon_t$  follows normal distribution with mean 0 and standard deviation  $\sigma_{\epsilon}$ .

bounded were much more gradual and similar to historical trends. SRR-AR1 and SRR-cut-off produced similar trends of productivity, recruitment, and SSB, although the projections by SRR-cut-off were kept as constant at historical boundaries. SRR-bounded also produced variations within historical boundaries but showed different trends than those generated by SRR-AR1 and SRR-cut-off.

**Simulation study**

When the productivity had high-frequency variations without long-term trend (stochastic variations), all seven methods produced similar levels of MSY,  $F_{MSY}$ , and  $B_{MSY}$ . The reference points produced by SRR-resample, SRR-AR1, SRR-cut-off, and SRR-bounded were slightly greater than those generated by SRR-whole, SRR-recent, and SRR-noise (Figure 4).

When the productivity exhibited low-frequency and large-magnitude variations with increasing trend (upward shift), decreasing trend (downward shift), and U-shape trend (collapse and recover), the seven methods produced drastically different reference points. SRR-whole, SRR-AR1, SRR-cut-off, and SRR-bounded produced smaller MSY and  $F_{MSY}$  than SRR-noise and SRR-resample, yet no consistent pattern was found for  $B_{MSY}$  (Figure 4). The MSY,  $F_{MSY}$ , and  $B_{MSY}$  produced by SRR-recent were greater than SRR-whole when productivity was increasing,

and the opposite was found when productivity was decreasing (Figure 4). When the productivity showed U-shape variation, there were no consistent differences of reference points between SRR-recent and SRR-whole (Figure 4).

**Case studies**

The SRRs of 3NO cod and 3LNO plaice showed strong temporal variations (Supplementary Figure S2), suggesting the existence of non-stationary SRRs. For both stocks, *Ricker.tv* had much better fit than *Ricker* (Figure 5). Population productivity (represented by  $\alpha_t$  in *Ricker.tv*) decreased drastically during the 1980s and reached very low levels around 1990 for both 3NO cod and 3LNO plaice (Figure 5). Since then, the productivity of both stocks showed cyclic variations, though generally remaining lower than the historical productivity in the 1960s and 1970s (Figure 5).

For 3NO cod and 3LNO plaice, reference points varied greatly depending on the method used to model SRRs. For both stocks, SRR-noise and SRR-resample produced greater MSY and  $F_{MSY}$  than other methods, while SRR-recent generated the smallest MSY and  $B_{MSY}$  (Table 5). SRR-AR1, SRR-cut-off, and SRR-bounded produced smaller values of MSY,  $F_{MSY}$ , and  $B_{MSY}$  than SRR-whole, SRR-noise, and SRR-resample for 3NO cod, but not 3LNO plaice (Table 5). When using methods that produced time-varying SRR projections, the relationship between fishing mortality and yield was asymmetric: yield showed gradual increase and sharp decrease with increasing fishing mortality (Figure 6). In addition, the relationships between fishing mortality and yield or biomass were more variable for SRR-AR1, SRR-cut-off, and SRR-bounded than for SRR-noise and SRR-resample (Figures 6 and 7).

**Discussion**

**Recruitment projection under different SRR assumptions**

Recruitment projection is a long-standing challenge in fisheries science (Subbey et al., 2014), and numerous parametric and non-parametric methods have been developed (Maunder and Thorson, 2019). In parametric methods, recruitment is typically projected by either using a deterministic stock–recruitment model or adding stochastic residuals to certain forms of stock–recruitment models, e.g. residuals sampled from predictive distributions are added to a deterministic stock–recruitment model

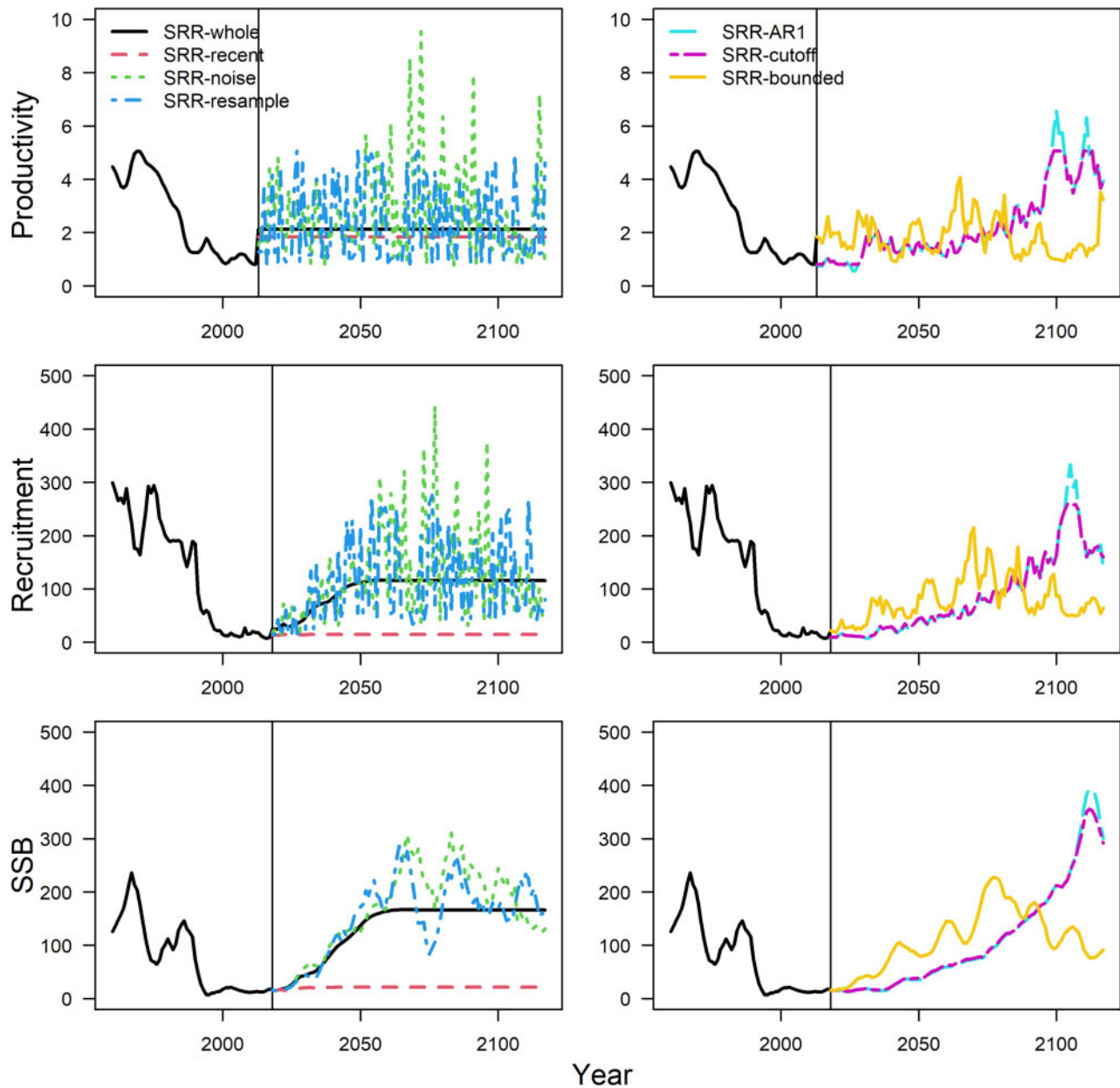


**Figure 3.** Temporal variations in productivity, recruitment, and SSB when using seven methods to model SRRs. This is drawn from one simulation run for 3LNO plaice, and the general patterns of variation are consistent among simulation runs. The vertical lines separate the historical and projected periods.

(Methot and Wetzel, 2013; ICES Advisory Committee, 2014). However, few attempts have been made to integrate time-varying parameters of SRR into recruitment projections. We compared seven methods to project recruitment by assuming different temporal variations of SRR parameters. Deterministic projections (SRR-whole and SRR-recent) led to constant recruitment in the long-term, stochastic projections (SRR-noise and SRR-resample) generated highly stochastic recruitment with strong annual fluctuations, and autocorrelated projections (SRR-AR1, SRR-cut-off, and SRR-bounded) produced recruitment that varies gradually over time. Among the three autocorrelated projection methods, SRR-AR1 could produce recruitment exceeding historical boundaries, and SRR-cut-off tended to generate constant recruitment at

historical boundaries. If we assume the future dynamics of recruitment resemble the past, SRR-bounded has the most realistic projections in terms of similarity in temporal trend and exclusion of extreme values. This projection method may be a useful addition to existing simulation packages used to calculate MSY-based reference points, e.g. Stock Synthesis and Eqsim (Methot and Wetzel, 2013; ICES Advisory Committee, 2014). Meanwhile, it is important to keep in mind that the future dynamics of fish populations may produce recruitment exceeding historical bounds, in which case the SRR-AR1 approach could also be a valid option.

Although we restrict our study on time-varying SRRs, it is important to note that other aspects of fish population dynamics

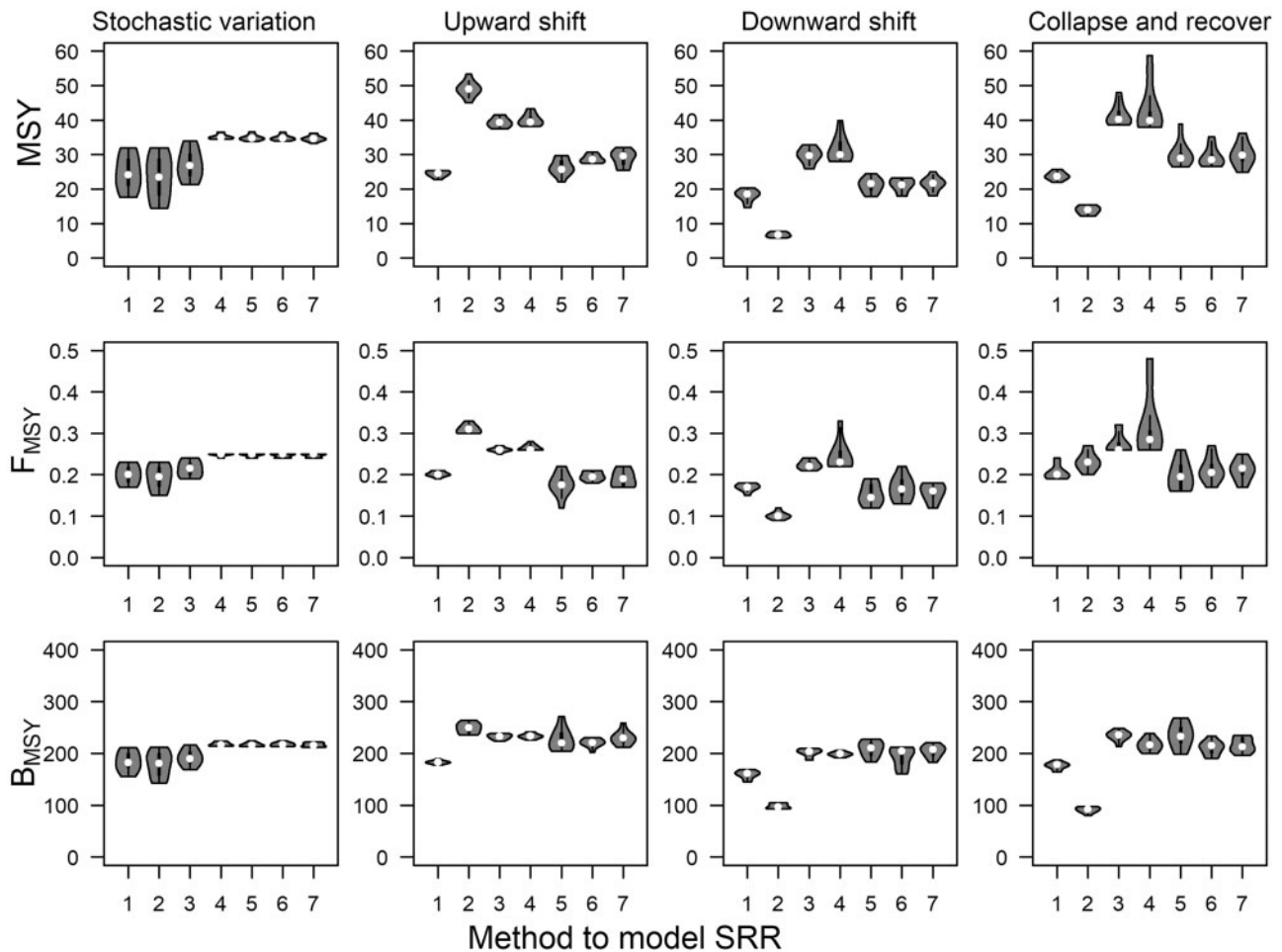


**Figure 4.** Violin plot of the  $MSY$ ,  $F_{MSY}$ , and  $B_{MSY}$  derived from seven methods to model SRRs under four scenarios of operating module. Each scenario is repeated for 100 times. Scenario 1: stochastic variation; scenario 2: upward shift; scenario 3: downward shift; and scenario 4: collapse and recover. Method 1: SRR-whole; method 2: SRR-recent; method 3: SRR-noise; method 4: SRR-resample; method 5: SRR-AR1; method 6: SRR-cut-off; and method 7: SRR-bounded.

(e.g. maturation and growth) may also change over time (Thorson *et al.*, 2015). The projection method used in this paper (e.g. SRR-bounded) can also be applied to account for time-varying maturity, growth, and natural mortality. For example, time-varying growth can be modelled using bounded AR1 method (i.e. the method used in SRR-bounded) to project time-varying growth parameter (i.e. parameter  $k$ ) of the von Bertalanffy growth model. In addition, the variations in multiple population traits may lead to additive, synergic, or agnostic effects on management reference points, and it remains a significant challenge to account for multiple time-varying population traits in fisheries management. Hence, further studies may benefit from exploring the interactions among multiple time-varying population traits.

#### MSY-based reference points under different SRR assumptions

Both simulation and case studies indicate that stochastic SRRs tend to produce greater  $MSY$  and  $F_{MSY}$  than autocorrelated and constant SRRs when the true population productivity has low-

frequency and large-magnitude variations. Consistently, stochastic SRRs tend to generate greater long-term recruitment than autocorrelated and constant SRRs, especially when there are strong variations in productivity (Supplementary Figure S3). Hence, in ecosystems exhibiting slow and large variations, using stochastic SRRs to calculate reference points may increase the risk of overexploitation. Meta-analysis also indicates that the recovery probability of fish populations is lower in dynamic models with autocorrelated variation in productivity (Britten *et al.*, 2017), and a lower constant harvest rate is recommended for fish populations experiencing low-frequency environmental variations (Polovina, 2005). In addition, we find that autocorrelated SRRs produce more variable relationships between fishing mortality and yield, and these relationships are asymmetric with steeper decline in yield when fishing mortality exceeds  $F_{MSY}$ . This suggests higher risks of losing yield by going beyond than below  $F_{MSY}$ . Therefore, more conservative harvest strategies (e.g. lower fishing mortality) should be considered in highly dynamic ecosystems, which is consistent with the common practice of using  $F_{MSY}$  as a limit rather than target under any PA framework for fisheries management. In accordance with the need for reduced fishing

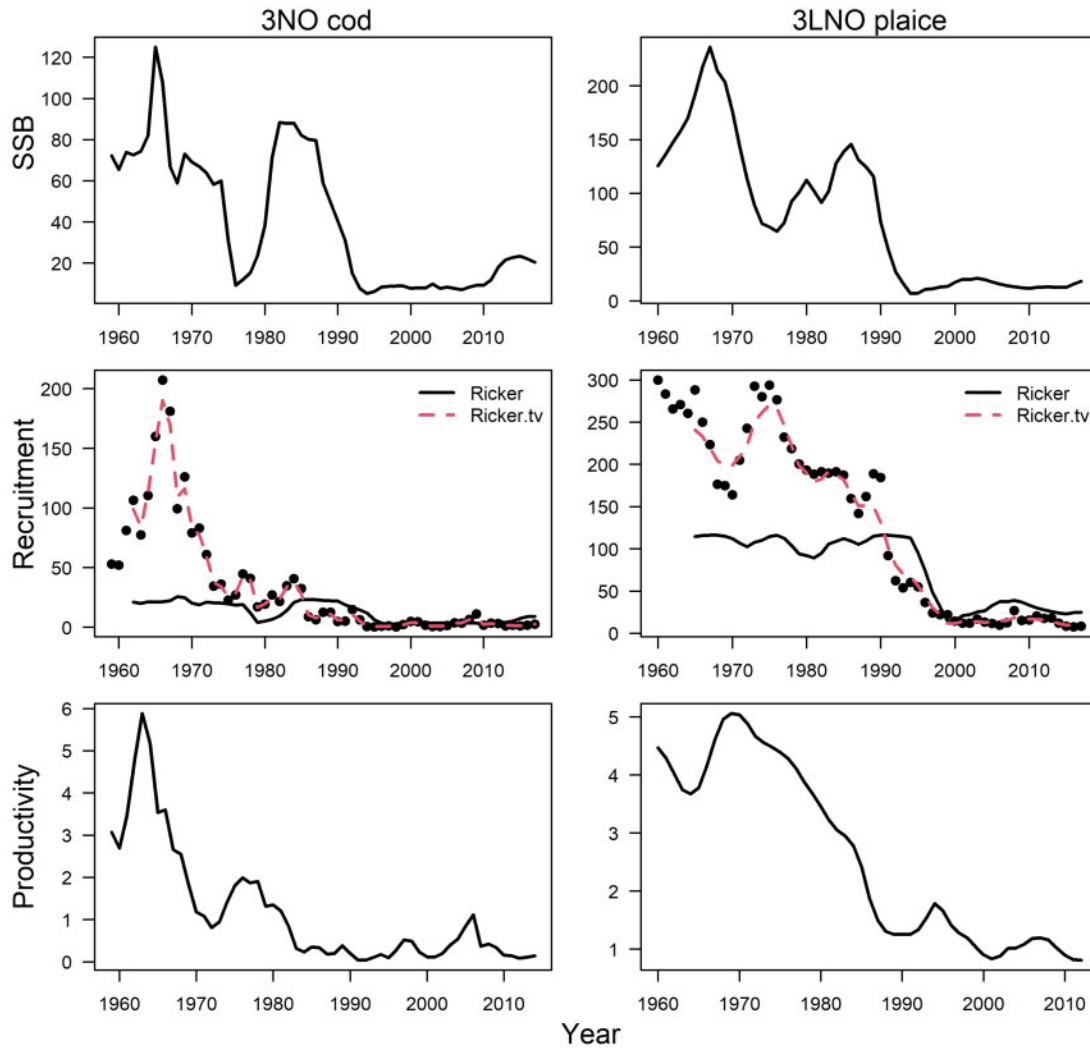


**Figure 5.** The temporal variations in SSB, recruitment and productivity of 3NO cod and 3LNO plaice. In the middle panels, dots are the observed recruitment, black solid lines are the recruitment predicted by *Ricker* model, and red dashed lines are the recruitment predicted by *Ricker.tv* model.

**Table 5.**  $MSY$ ,  $F_{MSY}$ , and  $B_{MSY}$  of 3NO cod and 3LNO plaice using seven methods to model SRRs.

Method	3NO cod			3LNO plaice		
	MSY	$F_{MSY}$	$B_{MSY}$	MSY	$F_{MSY}$	$B_{MSY}$
SRR-whole	14.85	0.15	146.73	14.74	0.20	162.74
SRR-recent	1.35	0.15	13.29	1.63	0.17	20.37
SRR-noise	33.99	0.24	216.98	19.97	0.24	192.77
SRR-resample	24.99	0.27	143.34	20.01	0.24	193.06
SRR-AR1	7.10	0.08	127.14	13.02	0.16	169.92
SRR-cut-off	7.02	0.08	129.38	14.24	0.16	189.87
SRR-bounded	5.36	0.06	129.56	13.39	0.14	196.32

mortality in highly dynamic ecosystems, lower fishery yield should also be anticipated. The long-term sustainable yield derived from stochastic fishery models may not be achievable under autocorrelated environmental variations. Fishery managers should understand and communicate this uncertainty to mitigate

negative impacts and to manage the socioeconomic expectations of the fishing industry and fishing communities.

Our case study is based on 3NO cod and 3LNO plaice, both of which experienced a prolonged period of low population productivity in recent decades. Although a large number of global fisheries show similar collapse in fish population productivity (Vert-Pre *et al.*, 2013; Szuwalski *et al.*, 2015; Zhang, 2020), there are fish populations that exhibit rapid recovery or even persistent increase in productivity (Clements *et al.*, 2019). Nevertheless, our simulation study demonstrated that our conclusions are robust regardless of the population experiencing increasing, decreasing, or recovering productivity. Meanwhile, we did find differences between simulation and case studies regarding the difference between constant and autocorrelated SRRs. The constant SRRs produced greater  $MSY$  and  $F_{MSY}$  than autocorrelated SRRs in the case study of 3NO cod, which was not detected in the simulation. Hence, case-specific simulations are needed to fully understand the explicit impacts of SRR assumptions on  $MSY$ -based reference points in empirical studies.



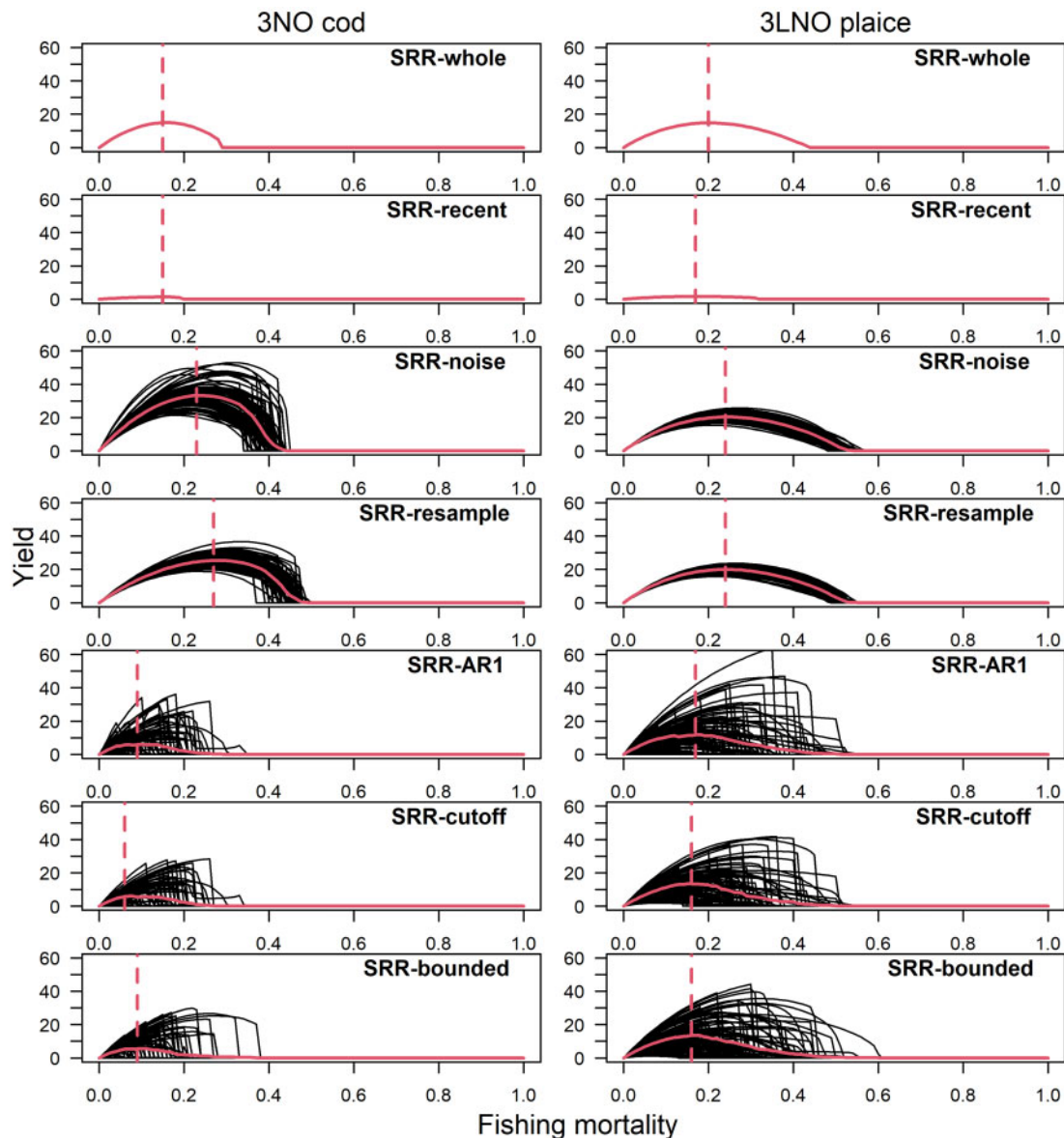


**Figure 6.** The relationship between fishing mortality and long-term yield (mean yield over last 100 years of each simulation run) for 3NO cod and 3LNO plaice when using seven methods to model SRRs. The black lines are the relationships over 100 repetitions (i.e. first layer of the simulation framework shown in [Supplementary Figure S1](#)), the red solid lines are the mean relationship averaged over 100 repetitions, and the vertical red dashed lines are the  $F_{MSY}$ .

### Low-frequency and large-magnitude variations of population dynamics

One key finding of our study is that the effects of SRR assumptions on MSY-based reference points are most significant when the true population dynamics show low-frequency and large-magnitude variations. This type of variation is likely to occur when there is ecosystem regime shift or strong climate effects. For example, strong variations in the SRRs of yellow perch (*Perca flavescens*) are closely related to ecosystem regime shifts of Lake Erie due to invasive species ([Zhang et al., 2018](#)). Multidecadal variations in the recruitment of sardine (*Sardinops sagax*) and anchovy (*Engraulis mordax*) coincide with the periodic dynamics of Pacific Decadal Oscillation ([Chavez et al., 2003](#)). Cumulative evidence suggests that low-

frequency and large-magnitude variations in SRRs are common among global fish stocks ([Vert-Pre et al., 2013](#); [Minto et al., 2014](#); [Szuwalski et al., 2015](#)), emphasizing the necessity to account for such non-stationary dynamics when setting management reference points.

In the case study, we detected strong temporal variations in the SRRs of 3NO cod and 3LNO plaice. [Morgan et al. \(2014\)](#) also reported high- and low-productivity periods for these two fish stocks but did not examine the annual variation in SRRs. Using a state-space modelling approach, we estimated the annual variation in population productivity. There was a synchronized collapse of both stocks during the 1980s and further decline in the early 1990s (especially 3NO cod), corresponding to a period of ecosystem change in the Northwest Atlantic ([Greene and](#)

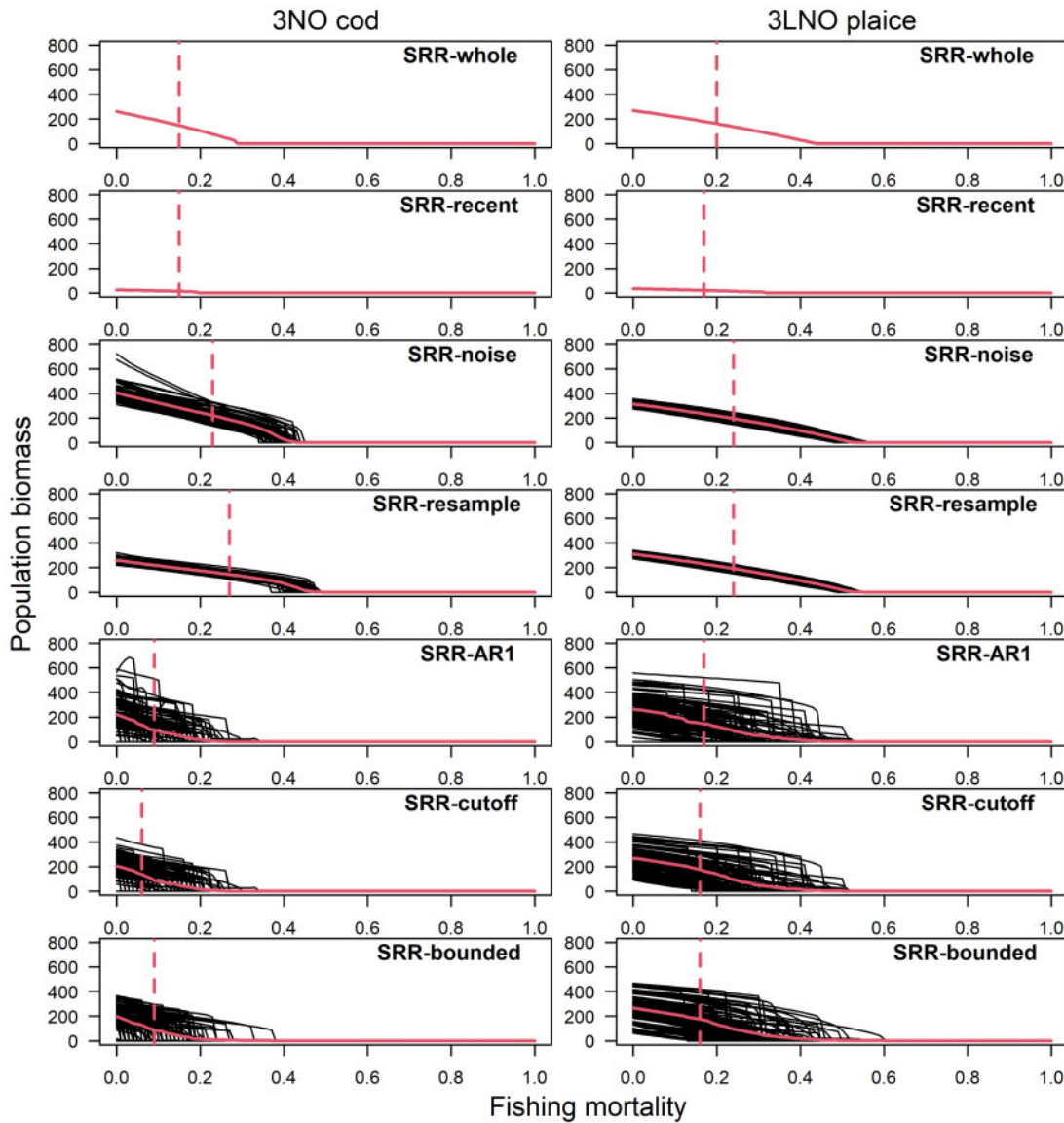


**Figure 7.** The relationship between fishing mortality and long-term population biomass (mean population biomass over last 100 years of each simulation run) for 3NO cod and 3LNO plaice when using seven methods to model SRRs. The black lines are the relationships over 100 repetitions (i.e. first layer of the simulation framework shown in [Supplementary Figure S1](#)), the red solid lines are the mean relationship averaged over 100 repetitions, and the vertical red dashed lines are the  $F_{MSY}$ .

[Pershing, 2007](#); [Pedersen et al., 2017](#)). The collapse of multiple fish stocks was observed during this period, accompanied with dramatic changes in fish community structure ([Dempsey et al., 2017](#); [Pedersen et al., 2017](#)). Although the explicit mechanisms causing these ecosystem changes are still elusive, it is speculated that both climatic and anthropogenic (e.g. overfishing) factors are important causes ([Kumar et al., 2019](#); [Zhang et al., 2020](#)). Therefore, the time-varying SRRs of 3NO cod and 3LNO plaice are likely to be associated with low-frequency environmental and/or anthropogenic effects, and autocorrelated SRRs are more realistic than deterministic or stochastic SRRs. Hence, we recommend using autocorrelated SRRs when setting MSY-based reference points for these two stocks and others that also show low-frequency and large-magnitude variations in SRRs.

### Supplementary data

[Supplementary material](#) is available at the *ICESJMS* online version of the manuscript.

### Acknowledgements

We thank the editor and two anonymous reviewers for their insightful comments that have improved the manuscript. We thank all the Fisheries and Oceans Canada sea-going staff involved in the collection and processing of the data used in the assessments of these stocks. We thank Noel G. Cadigan and Nan Zheng from Fisheries and Marine Institute of Memorial University for their insightful comments and contribution to the methodology development.

## Funding

This work was supported by the start-up fund of Fisheries and Marine Institute of Memorial University of Newfoundland, Ocean Choice International Junior Industry Research Chair Grant and research funding provided by the Ocean Frontier Institute through an award from the Canada First Research Excellence Fund.

## Data availability statement

Data used in this paper are available from the stock assessment reports of 3NO cod and 3LNO plaice (Rideout *et al.*, 2018; Wheeland *et al.*, 2018).

## References

- Beverton, R. J. H., and Holt, S. J. 1957. On the Dynamics of Exploited Fish Populations. Her Majesty's Stationery Office. 533 pp.
- Britten, G. L., Dowd, M., Kanary, L., and Worm, B. 2017. Extended fisheries recovery timelines in a changing environment. *Nature Communications*, 8: 15325.
- Chavez, F. P., Ryan, J., Lluch-Cota, S. E., and Niquen, C. M. 2003. From anchovies to sardines and back: multidecadal change in the Pacific Ocean. *Science*, 299: 217–221.
- Clements, C. F., McCarthy, M. A., and Blanchard, J. L. 2019. Early warning signals of recovery in complex systems. *Nature Communications*, 10: 1681.
- Dempsey, D. P., Koen-Alonso, M., Gentleman, W. C., and Pepin, P. 2017. Compilation and discussion of driver, pressure, and state indicators for the Grand Bank ecosystem, Northwest Atlantic. *Ecological Indicators*, 75: 331–339.
- Greene, C. H., and Pershing, A. J. 2007. Climate drives sea change. *Science*, 315: 1084–1086.
- Hidalgo, M., Olsen, E. M., Ohlberger, J., Saborido-Rey, F., Murua, H., Piñeiro, C., and Stenseth, N. C. 2014. Contrasting evolutionary demography induced by fishing: the role of adaptive phenotypic plasticity. *Ecological Applications*, 24: 1101–1114.
- Holt, S. J. 2020. Becoming a marine scientist: helped by a daily quota of three lumps of coal. *ICES Journal of Marine Science*, 77: 463–468.
- ICES Advisory Committee. 2014. Report of the Joint ICES-MYFISH Workshop to consider the basis for FMSY ranges for all stocks (WKMSYREF3), 17–21 November 2014, Charlottenlund, Denmark. ICES Document CM 2014/ACOM: 64. 156 pp.
- Klaer, N. L., O'Boyle, R. N., Deroba, J. J., Wayte, S. E., Little, L. R., Alade, L. A., and Rago, P. J. 2015. How much evidence is required for acceptance of productivity regime shifts in fish stock assessments: are we letting managers off the hook? *Fisheries Research*, 168: 49–55.
- Kristensen, K., Nielsen, A., Berg, C. W., Skaug, H., and Bell, B. M. 2016. TMB: automatic differentiation and Laplace approximation. *Journal of Statistical Software*, 70: 1–21.
- Kumar, R., Cadigan, N. G., and Morgan, J. M. 2019. Recruitment synchrony in spatially structured Newfoundland and Labrador populations of American plaice (*Hippoglossoides platessoides*). *Fisheries Research*, 211: 91–99.
- Mangel, M., Maccall, A. D., Brodziak, J., Dick, E. J., Forrest, R. E., Pourzand, R., and Ralston, S. 2013. A perspective on steepness, reference points, and stock assessment. *Canadian Journal of Fisheries and Aquatic Sciences*, 70: 930–940.
- Maunder, M. N., and Thorson, J. T. 2019. Modeling temporal variation in recruitment in fisheries stock assessment: a review of theory and practice. *Fisheries Research*, 217: 71–86.
- Method, R. D., and Wetzel, C. R. 2013. Stock synthesis: a biological and statistical framework for fish stock assessment and fishery management. *Fisheries Research*, 142: 86–99.
- Minto, C., Flemming, J. M., Britten, G. L., and Worm, B. 2014. Productivity dynamics of Atlantic cod. *Canadian Journal of Fisheries and Aquatic Sciences*, 71: 203–216.
- Morgan, M. J., Shelton, P. A., and Rideout, R. M. 2014. Varying components of productivity and their impact on fishing mortality reference points for Grand Bank Atlantic cod and American plaice. *Fisheries Research*, 155: 64–73.
- Pedersen, E. J., Thompson, P. L., Ball, R. A., Fortin, M.-J., Gouhier, T. C., Link, H., Moritz, C., *et al.* 2017. Signatures of the collapse and incipient recovery of an overexploited marine ecosystem. *Royal Society Open Science*, 4: 170215.
- Peterman, R. M., and Dorner, B. 2012. A widespread decrease in productivity of sockeye salmon (*Oncorhynchus nerka*) populations in western North America. *Canadian Journal of Fisheries and Aquatic Sciences*, 69: 1255–1260.
- Polovina, J. J. 2005. Climate variation, regime shifts, and implications for sustainable fisheries. *Bulletin of Marine Science*, 76: 233–244.
- Ricker, W. E. 1954. Stock and recruitment. *Journal of the Fisheries Research Board of Canada*, 11: 559–623.
- Rideout, R. M., Rogers, B., and Ings, D. W. 2018. An assessment of the cod stock in NAFO Divisions 3NO. NAFO Scientific Council Research Document, 2018/028.
- Subbey, S., Devine, J. A., Schaarschmidt, U., and Nash, R. D. M. 2014. Modelling and forecasting stock–recruitment: current and future perspectives. *ICES Journal of Marine Science*, 71: 2307–2322.
- Szuwalski, C. S., and Hollowed, A. B. 2016. Climate change and non-stationary population processes in fisheries management. *ICES Journal of Marine Science*, 73: 1297–1305.
- Szuwalski, C. S., Vert-Pre, K. A., Punt, A. E., Branch, T. A., and Hilborn, R. 2015. Examining common assumptions about recruitment: a meta-analysis of recruitment dynamics for worldwide marine fisheries. *Fish and Fisheries*, 16: 633–648.
- Thorson, J. T., Monnahan, C. C., and Cope, J. M. 2015. The potential impact of time-variation in vital rates on fisheries management targets for marine fishes. *Fisheries Research*, 169: 8–17.
- Vert-Pre, K. A., Amoroso, R. O., Jensen, O. P., and Hilborn, R. 2013. Frequency and intensity of productivity regime shifts in marine fish stocks. *Proceedings of the National Academy of Sciences of the United States of America*, 110: 1779–1784.
- Walters, C. J. 1987. Nonstationarity of production relationships in exploited populations. *Canadian Journal of Fisheries and Aquatic Sciences*, 44: s156–165.
- Wheeland, L., Dwyer, K., Morgan, J., Rideout, R., and Rogers, R. 2018. Assessment of American plaice in Div. 3LNO. NAFO Scientific Council Research Document, 2018/039.
- Wutzler, T. 2018. logitnorm: Functions for the Logitnormal Distribution. R package version 0.8.37.
- Zhang, F. 2020. Early warning signals of population productivity regime shifts in global fisheries. *Ecological Indicators*, 115: 106371.
- Zhang, F., Reid, K. B., and Nudds, T. D. 2018. Ecosystem change and decadal variation in stock–recruitment relationships of Lake Erie yellow perch (*Perca flavescens*). *ICES Journal of Marine Science*, 75: 531–540.
- Zhang, F., Rideout, R. M., and Cadigan, N. G. 2020. Spatiotemporal variations in juvenile mortality and cohort strength of Atlantic cod (*Gadus morhua*) off Newfoundland and Labrador. *Canadian Journal of Fisheries and Aquatic Sciences*, 77: 625–635.